Energy Transfer Dynamics of Nanocrystal−Polymer Composites

Jamie H. Warner,* Andrew R. Watt,* Elizabeth Thomsen, Norman Heckenberg, Paul Meredith, and Halina Rubinsztein-Dunlop

Center for Biophotonics and Laser Science, Center for Quantum Computer Technology, School of Physical Sciences, The University of Queensland, Brisbane, QLD 4072, Australia

Received: December 1, 2004; In Final Form: January 30, 2005

Steady-state and time-resolved photoluminescence spectroscopy are used to examine the photoluminescent properties of nanocrystal−polymer composites consisting of colloidal PbS nanocrystals blended with poly-(2-methoxy-5(2-ethylhexyloxy)-*p*-phenylene vinylene). Quenching of the emission from the conjugated polymer due to the PbS nanocrystals is observed along with band edge emission from the ligand capped PbS nanocrystals. A decrease in the photoluminescence lifetime of MEH-PPV is also observed in the thin film nanocrystal−polymer composite materials. Photoluminescence excitation spectroscopy of the PbS nanocrystal emission from the composite shows features attributed to MEH-PPV providing evidence of a Förster transfer process.

1. Introduction

Conjugated polymers have attracted a great deal of interest since their discovery in the 1970s, especially in a variety of photonics and optoelectronic applications such as electroluminescence,[1,2] photovoltaics,[3−5] and optical sensors.[4] The family of poly(*p*-phenylenevinylene) (PPV) derivative conjugated polymers combine semiconducting electronic properties with high room-temperature photoluminescence quantum yields (QY ∼35%) and strong nonlinear optical processes.[6]

Blending conjugated polymers with materials, such as semiconductor nanocrystals (NCs) and C60, has been found to enhance the performance of optoelectronic devices.[1−5,7,8] The conjugated polymer studied here is poly(2-methoxy-5-(2-ethylhexyloxy)-*p*-phenylene vinylene) (MEH-PPV), shown in Figure 1, which is blended with colloidal PbS semiconductor NCs to form a nanocrystal:polymer (NC:P) composite. Composites of this nature have recently been used as the active area in electroluminescent and photovoltaic devices, warranting further studies into their optical properties.[1,2,4,9−11]

The choice of conducting polymer is important if coupling of the nanocrystal and polymer is required, as recently demonstrated by MacDonald et al.[9] In a photovoltaic device the composite material requires a band alignment such that the ionization potential of the polymer lies closer to vacuum than that of the nanocrystal allowing transfer of holes from nanocrystal to polymer. The bulk ionization potential of PbS is ∼4.95 eV and MEH-PPV has been reported to be between ∼4.9 and ∼5.1 eV.[12,13] This difference in ionization potential is small; however, MacDonald et al.[9] and our own group have observed enhanced spectroscopic properties in photovoltaic devices, which indicates electronic coupling between MEH-PPV and PbS nanocrystals. Typically the nanocrystals used in photovoltaic devices have no surface capping ligands or otherwise a short chain molecule such as octylamine is used.[3,9]

In NC:P composite electroluminescence devices the surface of the nanocrystals is generally capped with a ligand.[11] In PbS NCs a surface capping ligand is necessary to obtain direct band edge photoluminescence. To date, ligand capped PbS NCs incorporated into MEH-PPV composites have been limited to absorption band edges between 800 and 2000 nm.[2,4,9−11] This has restricted the photoluminescence from the PbS NCs in the NC:P composites to wavelengths longer than 1000 nm.[1,2,11] Here we prepare PbS NCs, using our previously reported synthesis that has shown the ability to tune the band edge between 600 and 900 nm and then incorporate these into MEH-PPV NC:P composites.

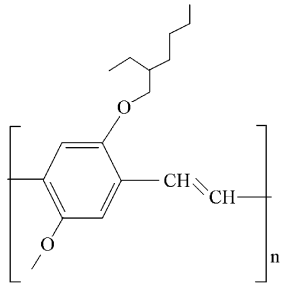

Figure 1. Schematic diagram of the base unit of the polymer MEH-PPV (poly(2-methoxy-5-(2′-ethylhexyloxy)-*p*-phenylene vinylene)).

Electroluminescent devices composed of blended PbS nanocrystals and MEH-PPV have shown the ability to generate emission from the PbS nanocrystals in the near-IR region (1.0−1.8 μm) with internal electroluminescent efficiencies up to 3.1%.[1,2] In this process the PbS nanocrystals were synthesized separately, using a colloidal organometallic route, and then mixed with MEH-PPV.[1,2] The colloidal nanocrystal synthesis typically involves a rapid injection of precursors into a hot coordinating solvent, which results in a short, single nucleation event that is followed by a slower growth period.[14]

The mean size of the PbS NCs can be adjusted by varying the temperature of the coordinating solvent before the precursors are injected. The current PbS:MEH-PPV electroluminescent devices use ligand capped PbS nanocrystals formed with TMS as the sulfur precursor, with a mean size tunable between 2 and 10 nm.[1,2,11] This limits the electroluminescence from the PbS nanocrystals blended with MEH-PPV to between 1 and 1.8 μm. However, recently we have shown that when TMS is replaced by H_2S gas the mean size of the PbS nanocrystals could

* Address correspondence to these authors. E-mail: warner@physics.uq.edu.au and watt@physics.uq.edu.au.

10.1021/jp044531b CCC: $30.25
Published on Web 04/09/2005

be tuned between 1 and 2 nm.[15] This resulted in photoluminescence from the PbS nanocrystals between 770 and 1000 nm.[15] Thus the emission from PbS NCs in PbS:MEH-PPV electroluminescent devices could potentially be extended to 770−1000 nm, further enhancing the spectral response of these devices.

Photovoltaic devices consisting of ligand capped PbS NCs blended with MEH-PPV have also been demonstrated with internal quantum efficiency of 3%.[9] Again the limitation of the spectral response of the photocurrent in these devices was determined by the size of the ligand capped PbS NCs. MEH-PPV has strong absorption between 400 and 600 nm and by blending it with 1−2 nm PbS NCs with an absorption band edge between 600 and 900 nm, it should be possible to extend the photocurrent's spectral response all the way to 600 nm. This would then provide photovoltaic devices composed of PbS NCs and MEH-PPV with possible photocurrent response covering the entire region from 2000 nm down to 400 nm.

There are generally two mechanisms used to describe the transfer of excitations between a conjugated polymer and a semiconductor nanocrystal, Dexter and Forster mechanisms.[3,11] The energy transfer rate of both mechanisms depends on the spectral overlap between the emission spectrum of the donor and the absorption spectrum of the acceptor and also on the separation between the donor and acceptor.[16,17] The Dexter mechanism relates to excitation transfer via an exchange process and is usually associated with the transfer of single charge carriers. It requires overlap of the wave functions between the two materials and is a short-range mechanism typically observed when NCs without a surface capping ligand are blended with conjugated polymers.[3] The rate of Dexter energy transfer, k_{ET}, is described by eq 1

$$k_{ET}(\text{Dexter}) = KJ \exp(-2R_{DA}/L) \quad (1)$$

where K describes specific orbital interactions, J is the spectral overlap integral, L is the van der Waals radii of the donor and acceptor, and R_{DA} is the donor−acceptor distance.

The Förster mechanism on the other hand is an energy transfer mechanism via the Coulomb dipole−dipole interaction[18] and the Förster energy transfer rate constant, k_{ET}, is given by eq 2

$$k_{ET}(\text{Förster}) = k(\kappa^2 k_d^\circ J(\epsilon_A)/R_{DA}^6) \quad (2)$$

where k is a constant influenced by experimental conditions (sample preparation, solvent index of refraction, etc.), κ is an orientation factor of dipoles, k_d° is the radiative rate constant of the donor from its excited state to ground state, R_{DA} is the donor−acceptor distance, and $J(\epsilon_A)$ is the spectral overlap integral.

Typically the transfer of energy via the Förster mechanism can occur over longer separation distances than the Dexter mechanism due to it being less sensitive to the donor−acceptor distance. Förster transfer of energy is often observed between conjugated polymers and ligand capped semiconductor nanocrystals.[1,2,11,19] The transfer of energy from MEH-PPV to the ligand-capped nanocrystals is the basic photophysics that underpins the performance of NC:P electroluminescent devices.[1,2,11] Improved performance of NC:P composite materials in optoelectronic devices requires further understanding of the transport processes occurring between the two materials.

Characteristics of Förster energy transfer from a donor to an acceptor are a decrease in the photoluminescence of the donor and a decrease in the excited-state lifetime of the donor and fluorescence from the acceptor.[18] Thus we expect the transfer of excitations from MEH-PPV to the ligand capped PbS NCs to quench the photoluminescence yield of MEH-PPV and consequently give rise to photoluminescence from the PbS NCs. A corresponding decrease should also be observed in the photoluminescence lifetime of MEH-PPV.

In this report we prepare 1 and 2 nm PbS NCs capped with oleic acid, blend them with MEH-PPV, and then form thin films similar to those used in the current PbS:MEH-PPV electroluminescent devices.[1,2] Steady state and time-resolved optical spectroscopy are used here to study these composite thin films to obtain a further understanding of their optical properties.

2. Experimental Section

The surface passivated PbS NCs were made according to the following procedure of Warner et al.:[15] In a continuously stirred sealed flask, a lead oleate precursor solution containing 0.1 g of lead acetate, 10 mL of *n*-decane, and 0.4 mL of oleic acid was heated to 120 °C for 20 min under a continuous flow of argon. Next the solution was cooled to 50 °C and 1 mL of H_2S gas was injected at a rate of 1×10^{-4} L/s into the gas phase of the sealed flask. PbS nanocrystal formation occurred within seconds of the complete injection of the H_2S gas and after 1 min the reaction was complete and the solution was subsequently cooled back to room temperature. This procedure produced a colloidal suspension of oleic acid capped PbS NCs with a mean size of approximately 1 nm and an absorption band edge at 630 nm. Two-nanometer PbS NCs with an absorption band edge at 770 nm were prepared by increasing the reaction temperature from 50 to 100 °C.

The PbS NCs were then precipitated out of solution by the addition of 5 mL of methanol and subjected to centrifuging for 10 min at 13 000 rpm. The supernatant was removed and the PbS NCs were redispersed in a viscous solution of MEH-PPV in chlorobenzene to form a NC:P colloidal suspension with various concentrations of 30% wt, 50% wt, 70% wt, and 90% wt of PbS NC, suitable for spin casting thin films of the composite material.

Room-temperature optical absorption spectra were obtained with a Perkin-Elmer Lambda 5 UV/vis spectrophotometer operating with the slits set to a 2 nm band-pass and 1 nm grating steps. Room-temperature photoluminescence (PL) spectra between 700 and 1000 nm were collected perpendicular to an excitation laser beam (532 nm CW), using a single lens, coupled into a single-grating (1200 g/mm) monochromator (Acton Research) with a silicon photodiode detector. UV−vis photoluminescence and photoluminescence excitation (PLE) spectroscopy were conducted with a commercial fluorimeter (Spex Fluoromax3). The slits for the excitation and detection channels were set to obtain a 3 nm band-pass. The PL and PLE spectra were corrected for the spectral response of the photomultiplier tube, excitation source, and diffraction grating.

Time-resolved photoluminescence spectroscopy was performed with a time-correlated single photon counting spectrometer (Picoquant Fluotime 200). For excitation a Titanium: Sapphire femtosecond laser was used (Spectra Physics Tsunami), operating with an 8 MHz pulse train with individual pulses having a duration of 70 fs at a wavelength of 800 nm. This was then frequency doubled with use of a nonlinear BBO crystal for single photon excitation at 400 nm.

3. Results and Discussion

A. Transmission Electron Microscopy. Synthesizing both 1 and 2 nm PbS NCs allows features observed in the optical spectra to be easily assigned to the PbS NCs rather than MEH-PPV and also demonstrates the ability to tune the optical

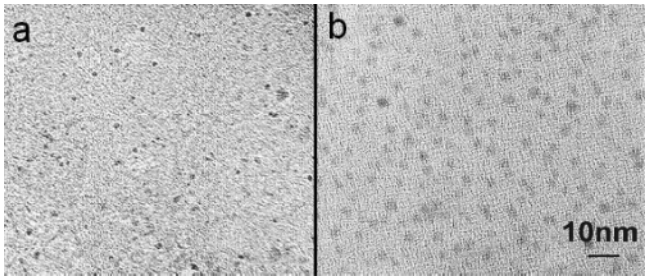

Figure 2. High-resolution transmission electron microscopy images of (a) 1 nm and (b) 2 nm PbS nanocrystals.

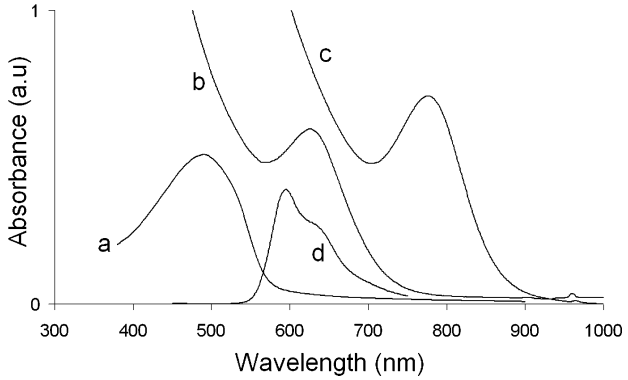

Figure 3. (a) Absorption spectrum of pristine MEH-PPV thin film. (b) Absorption spectrum of NC:P composite thin film with 50% wt 1 nm PbS NCs. (c) Absorption spectrum of NC:P composite thin film with 50% wt 2 nm PbS NCs. (d) Photoluminescence spectrum of pristine MEH-PPV thin film. All spectra have been normalized for clarity of presentation.

properties of the NC:P composites. The size and size distribution of the PbS nanocrystals were analyzed by using transmission electron microscopy before being blended with MEH-PPV. Figure 2 shows the high-resolution transmission electron microscopy (HRTEM) images of both the (a) 1 and (b) 2 nm PbS NCs synthesized at 50 and 100 °C, respectively. The HRTEM images show monodisperse samples of PbS nanocrystals were produced even for these very small sizes of 1−2 nm, similar to previous reports.[15]

B. Absorption Spectroscopy. Next we use absorption spectroscopy to show the PbS nanocrystals still exhibit a well-defined absorption band edge when blended with the conducting polymer. Figure 3 shows the absorption spectra of thin films of (a) pristine MEH-PPV, (b) 50% wt 1 nm PbS NC:P composite, and (c) 50% wt 2 nm PbS NC:P composite. The photoluminescence spectrum of a thin film of pristine MEH-PPV is also presented in Figure 3d and shows the overlap between the emission spectrum of MEH-PPV and the absorption spectra of the PbS NCs in the composite materials. All spectra in Figure 3 have been normalized for clarity of presentation. The two different NC:P composites in panels b and c of Figure 3 contain the two different sized PbS NCs (1 nm, 2 nm) which gives rise to different band edge peaks in the absorption spectra.[6,7,10] The NC:P composite with the 1 nm PbS NCs has a peak at 630 nm, while the NC:P composite with the 2 nm PbS NCs has a peak at 775 nm. These two peaks are associated with the lowest energy exciton transition $1s_e-1s_h$ in the PbS NCs and agree well with theoretical predictions for PbS NCs of the respective size.[20,21] The absorption spectrum of the pristine MEH-PPV thin film shown in Figure 3a has a peak at 490 nm, which is of higher energy than the band edge of the PbS NCs in the composite materials. The observation of well-defined absorption band gap peaks for the PbS NCs suggests that the monodisperse size distribution is retained after being blended with the polymer.

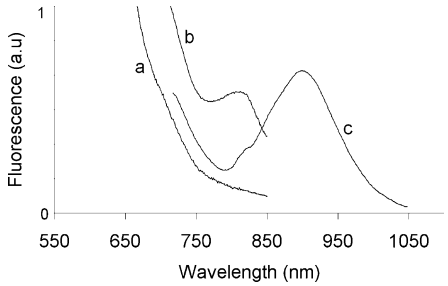

Figure 4. Photoluminescence spectrum (532 nm) of (a) a thin film of pristine MEH-PPV, (b) a NC:P composite thin film with 50% wt 1 nm PbS NCs, and (c) a NC:P composite thin film with 50% wt 2 nm PbS NCs.

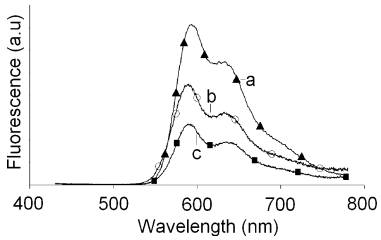

Figure 5. PL spectra (410 nm) for thin films of (a) pristine MEH-PPV, (b) a NC:P composite with 50% wt 1 nm PbS NCs, and (c) a NC:P composite with 50% wt 2 nm PbS NCs.

C. Photoluminescence Spectroscopy. The PbS NCs have their surfaces passivated by the oleic acid ligands and this allows radiative recombination to occur in the core of the PbS NCs. The oleic acid provides a barrier around the PbS NCs that increases the mean distance between the polymer and the PbS NCs and this effectively reduces the probability of a Dexter transfer process occurring between the MEH-PPV and the PbS NCs.[3] The Förster transfer of energy from MEH-PPV to the PbS NCs should result in radiative recombination in the PbS NCs. Figure 4 shows the 532 nm photoluminescence spectra for (a) a pristine MEH-PPV thin film, (b) a NC:P thin film composite with 50% wt 1 nm PbS NCs, and (c) a NC:P thin film composite with 50% wt 2 nm PbS NCs.

In Figure 4a,b, the two NC:P thin films showed the presence of an extra emission peak associated with the band edge radiative recombination from the PbS NCs.[15,20] The NC:P composite thin film with the 1 nm PbS NC band edge at 630 nm displays a band edge emission peak at 810 nm, while the NC:P composite thin film with the 2 nm PbS NC band edge absorption peak at 775 nm displays a band edge emission peak at 900 nm. The photoluminescence from the PbS NCs is attributed to direct exciton recombination[15] and suggests it may be possible to prepare electroluminescent devices that emit with wavelengths between 800 and 1000 nm. Currently, the shortest wavelength from an electroluminescent device that uses PbS NCs in a matrix of MEH-PPV is limited to approximately 1000 nm.[1,2]

Figure 5 shows the 410 nm PL spectra for thin films of (a) pristine MEH-PPV, (b) a NC:P composite with 50% wt 1 nm PbS NCs, and (c) a NC:P composite with 50% wt 2 nm PbS NCs. All three films display similar emission profiles from the MEH-PPV, which suggests a similar conformation of the conducting polymer in all cases. A change in the conformation of the MEH-PPV polymer chain can give rise to a variation in the PL spectrum and also modify the fluorescence decay time of the PL.[22] Thus we can be sure that the changes observed here are due to the presence of the PbS NCs and not from different conformations of the polymer.

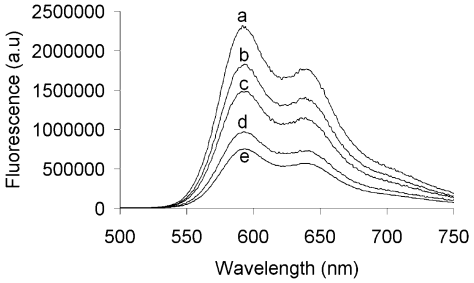

Figure 6. Photoluminescence spectra (410 nm) of MEH-PPV in composites consisting of PbS nanocrystals blended with MEH-PPV for increasing concentrations of PbS NCs: (a) 0% wt, (b) 30% wt, (c) 50% wt, (d) 70% wt, and (e) 90% wt.

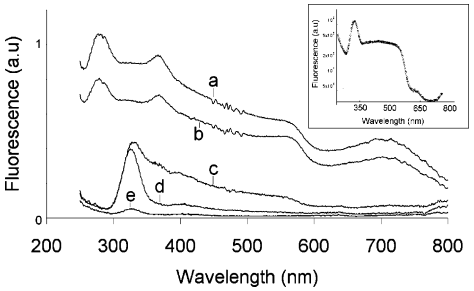

Figure 7. Photoluminescence excitation spectra (PLE) (820 nm) of PbS nanocrystals blended with MEH-PPV for decreasing concentrations: (a) 90% wt, (b) 70% wt, (c) 50% wt, (d) 30% wt, and (e) 0% wt. Top right inset is the 820 nm PLE spectra of a pristine MEH-PPV film (0%W).

A decrease in the photoluminescence yield of MEH-PPV for all NC:P composites was observed when compared to pure MEH-PPV. Quantitative measurement of the photoluminescence yield was obtained by taking into account the thickness and geometry of the samples, absorption of the excitation source, and reabsorption of the photoluminescence by the sample. Figure 6 shows the 410 nm photoluminescence spectra from MEH-PPV in 1 nm PbS NC:P composite thin films with increasing concentrations of 1 nm PbS NCs: (a) 0% wt, (b) 30% wt, (c) 50% wt, (d) 70% wt, and (e) 90% wt. As the concentration of the 1 nm PbS NCs increases from 0% wt to 90% wt the yield of the MEH-PPV emission decreases substantially. The decrease in the photoluminescence yield is attributed to quenching of the MEH-PPV by the PbS NCs in the composites, similar to other reports.[3] The PbS NCs quenched the photoluminescence of MEH-PPV by a factor of up to 3 in the 90% wt NC:P composites. The degree of quenching agrees well with other reports of NCs blended with MEH-PPV.[3]

D. Photoluminescence Excitation Spectroscopy. Photoluminescence excitation spectroscopy (PLE) was used to monitor the influence MEH-PPV absorption has on the band edge photoluminescence from 1 nm PbS NCs in NC:P composite thin films. Figure 7 shows the 820 nm PLE spectra of NC:P composite thin films with various concentrations of 1 nm PbS NCs: (a) 90% wt, (b) 70% wt, (c) 50% wt, (d) 30% wt, and (e) 0% wt. The top right inset in Figure 7 shows the 820 nm PLE spectrum of a pristine thin film of MEH-PPV exhibiting a clearly defined peak at 330 nm and a shoulder at 575 nm. Figure 7 shows that as the concentration of the PbS NCs decreases the photoluminescence at 820 nm also decreases in magnitude. This indicates that the emission being monitored comes primarily from the PbS NCs and not from the MEH-PPV.

When no PbS NCs are present in the NC:P, Figure 7e, the PLE consists of a small peak at 330 nm, which is attributed to MEH-PPV absorption (see the inset of Figure 7). When 30% wt 1 nm PbS NCs are added to the NC:P, Figure 7d, the PLE shows an increase in the magnitude of the photoluminescence, indicated by an increase in the PLE peak at 330 nm. When the concentration of the 1 nm PbS NCs is increased to 50% wt, Figure 7c, the PLE spectrum shows an increase in the photoluminescence from the absorbing state at 330 nm and also photoluminescence originating from absorption across a broader wavelength region (330−600 nm). A feature at 575 nm also becomes apparent for the 50% wt 1 nm PbS NCs in the NC:P composite and this is attributed to MEH-PPV absorption (see the inset of Figure 7). Thus at the two lowest concentrations (30% wt and 50% wt) of 1 nm PbS NCs in the NC:P composites, the PLE spectrum of the PbS NC band edge emission only shows features that correspond to MEH-PPV absorption (peak at 330 nm and a shoulder at 575 nm). This suggests that absorption by MEH-PPV leads to emission in the PbS NCs and provides strong evidence for the Förster transfer of energy from MEH-PPV to the PbS NCs in these NC:P thin films.

When the concentration of PbS NCs in the NC:P thin films is increased to 70% wt, Figure 7b, the peak in the PLE spectrum at 330 nm is no longer prominent, but the shoulder at 575 nm is retained. New peaks are now observed in the PLE spectrum at 700, 370, and 280 nm, which can be attributed to the absorption from the $1s_e-1s_h$, $1s_e-1p_h$, and $1p_e-p_h$ direct exciton transitions respectively in the PbS NCs.[20,21] These features are also observed in the PLE spectrum of the NC:P film with 90% wt 1 nm PbS NCs, Figure 7a. Thus at high PbS NC concentration it seems that the photoluminescence originates from both PbS NC absorption and also Förster transfer of energy from MEH-PPV.

These PLE results suggest that there exists an optimum concentration of PbS NCs in NC:P composite thin films that gives the highest magnitude of emission from the PbS NCs that is derived primarily from the Förster transfer of energy from MEH-PPV rather than direct absorption and recombination in the PbS NCs themselves. Here we found this value to be approximately 50% wt of 1 nm PbS NCs in MEH-PPV and when the concentration was lower than this the magnitude of PbS NC band edge photoluminescence decreased. When the concentration of 1 nm PbS NCs in MEH-PPV was higher than 50% wt the emission from the PbS NCs was related to both the direct absorption and recombination in the PbS NCs as well as the Förster transfer of energy from MEH-PPV to the PbS NCs.

E. Time-Resolved Photoluminescence Spectroscopy. Figure 8 shows the photoluminescence lifetime decays measured at 600

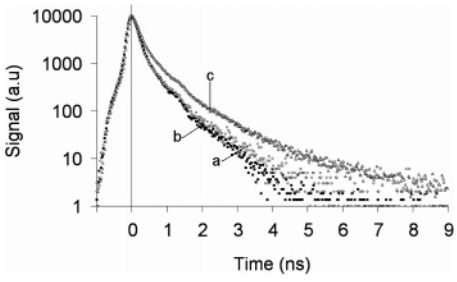

Figure 8. Photoluminescence lifetime decay (600 nm) of (a) a 90% wt 1 nm PbS NC NC:P thin film, (b) a 90% wt 2 nm PbS NC NC:P thin film, and (c) a pristine MEH-PPV thin film.

TABLE 1: Summary of Amplitudes (α) and Lifetime Components (τ) for Both Pristine MEH-PPV and 90% wt 1 nm PbS NC:P Thin Films Measured at 600 nm

	α_1	τ_1	α_2	τ_3	α_3	τ_3
MEH-PPV	568114	0.0186 ns	30686	0.235 ns	1536	1.109 ns
NC:P	553049	0.0189 ns	35529	0.163 ns	2635	0.742 ns

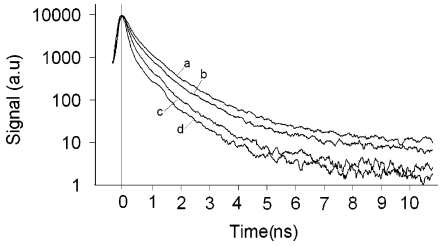

Figure 9. Photoluminescence lifetime decays (600 nm) for thin film composites of PbS nanocrystals blended with MEH-PPV with PbS NC concentrations of (a) 0% wt, (b) 30% wt, (c) 50% wt, and (d) 70% wt.

nm for (a) 90% wt 1 nm PbS NC:P composite thin film, (b) 90% wt 2 nm NC:P composite thin film, and (c) a pristine MEH-PPV thin film. Clearly the lifetime of the NC:P thin film composites is shorter than that of the pristine thin film of MEH-PPV, similar to other reports.[19] Analysis of the photoluminescence lifetime decays revealed a three-component exponential fit, summarized in Table 1. The dominating component at all emission wavelengths was below the resolution of our instrument ($\tau_1 < 40$ ps). The other two components for the emission at 600 nm were measured to be $\tau_2 = 0.23$ ns and $\tau_3 = 1.1$ ns, respectively, for the thin film of pristine MEH-PPV. These results agree well with other reports of the photoluminescence lifetime decays and the proposed energy relaxation mechanisms for MEH-PPV.[22] However, the NC:P composite thin films showed a 40% decrease in lifetime of the two longer components with $\tau_2 = 0.16$ ns and $\tau_3 = 0.74$ ns when compared to that of pristine MEH-PPV at both emission wavelengths of 600 and 640 nm.

Figure 9 shows how the photoluminescence lifetime decays of the NC:P composite thin films, measured at 600 nm, vary as the concentration of the 1 nm PbS NCs is increased with (a) 0% wt, (b) 30% wt, (c) 50% wt, and (d) 70% wt. As the concentration increases the decay of the MEH-PPV in the NC:P composite thin film becomes more rapid. This indicates the presence of a new relaxation process for MEH-PPV (i.e., Förster energy transfer to PbS NCs) that becomes more dominant as the concentration is increased. The decrease in the photoluminescence lifetime of the NC:P composites as compared to that of pristine MEH-PPV provides further evidence of Förster transfer from the MEH-PPV to the PbS NCs in the composite thin films. However, it is difficult to determine the contribution the excitation transfer via the Dexter mechanism between the MEH-PPV and the PbS NCs has on the photoluminescence lifetime decay. This will be probed deeper in future investigations.

4. Conclusion

In conclusion, we have shown that ligand capped 1−2 nm PbS NCs with band edges tunable between 630 and 810 nm can be incorporated into thin film NC:P composites with MEH-PPV and still retain their narrow absorption and photoluminescence spectra. Photoluminescence excitation spectroscopy of the emission from the PbS NC band edge in the NC:P thin films showed absorption features attributed to MEH-PPV and provided strong evidence for the Förster transfer of energy from MEH-PPV to the ligand capped PbS NCs. Quenching of the MEH-PPV emission by the PbS NCs was also observed in the NC:P films and was found to be dependent upon the concentration of PbS NCs. Finally photoluminescence lifetime decays of the MEH-PPV emission showed a significant decrease in the composite materials as compared to MEH-PPV. This decrease in the photoluminescence lifetime of MEH-PPV also indicates an interaction between the polymer and the PbS NCs in these composite materials.

Acknowledgment. We are grateful to the Australian Research Council for the financial support of the research conducted herein.

References and Notes

(1) Bakueva, L.; Musikhin, S.; Hines, M.; Chang, T.; Tzolov, M.; Scholes, G.; Sargent, E. *Appl. Phys. Lett.* **2003**, *17*, 263.
(2) Bakueva, L.; Konstantatos, G.; Levina, L.; Musikhin, S.; Sargent, E. *Appl. Phys. Lett.* **2004**, *84*, 3459.
(3) Greenham, N.; Peng, X.; Alivisatos, A. *Phys. Rev. B* **1996**, *54*, 17628.
(4) McDonald, S. A.; Konstantatos, G.; Zhang, S.; Cyr, P. W.; Klem, E. J. D.; Levina, L.; Sargent, E. H. *Nat. Mater.* Published online 2005, http://dx.doi:10.1038/nmat1299.
(5) Halls, J. J. M.; Pichler, K.; Friend, R. H.; Moratti, S. C.; Holmes, A. B. *Appl. Phys. Lett.* **1996**, *22*, 3120.
(6) De Boni, L.; Andrade, A. A.; Correa, D. S.; Balogh, D. T.; Zilio, S. C.; Misoguti, L.; Mendonca, C. R. *J. Phys. Chem. B* **2004**, *108*, 5221.
(7) Brabec, C. J.; Sariciftci, S.; Hummelen, J. C. *Adv. Func. Mater.* **2001**, *11*, 15.
(8) Khöler, A.; dos Santos, D. A.; Beljonne, D.; Shuai, Z.; Bredas, J.-L.; Holmes, A. B.; Kraus, A.; Mullen, K.; Friend, R. H. *Nature* **1998**, *392*, 903.
(9) McDonald, S. A.; Cyr, P. W.; Levina, L.; Sargent, E. H. *Appl. Phys. Lett.* **2004**, *85*, 2089.
(10) Bakueva, L.; Konstantatos, G.; Musikhin, S.; Ruda, H. E.; Shik, A. *Appl. Phys. Lett.* **2004**, *85*, 3567.
(11) Chang, F.; Musikhin, S.; Bakueva, L.; Levina, L.; Hines, M.; Cyr, P.; Sargent, E. *Appl. Phys. Lett.* **2004**, *84*, 4295.
(12) Greenwald, Y.; Xu, X.; Fourmigue, M.; Srdanov, G.; Koss, C.; Wudl, F.; Heeger, A. J. *J. Polym. Sci. A* **1998**, *36*, 3115.
(13) Jin, S.-H.; Jang, M.-S.; Suh, H.-S.; Cho, H.-N.; Lee, J.-L.; Gal, Y.-S. *Chem. Mater.* **2002**, *14*, 643.
(14) Hines, M. A.; Scholes, G. D. *Adv. Mater.* **2003**, *15*, 1844.
(15) Warner, J. H.; Thomsen, E.; Watt, A. R.; Heckenberg, N. R.; Rubinsztein-Dunlop, H. *Nanotehcnology* **2005**, *16*, 175.
(16) http://www.iupac.org/goldbook/D01654.pdf.
(17) http://www.iupac.org/goldbook/F02488.pdf.
(18) Scholes, G. D. *Annu. Rev. Phys. Chem.* **2003**, *54*, 57.
(19) Anni, M.; Manna, L.; Cingloani, R.; Valerini, D.; Creti, A.; Lomascolo, M. *Appl. Phys. Lett.* **2004**, *85*, 4169.
(20) Wise, F. W. *Acc. Chem. Res.* **2000**, *33*, 773.
(21) Kang, I.; Wise, F. *J. Opt. Soc. Am. B* **1997**, *14*, 1632.
(22) Samuel, I.; Rumbles, G.; Collison, C.; Friend, R.; Moratti, S.; Holmes, A. *Synth. Met.* **1997**, *84*, 497.